

Numerical modeling of anomalous spatial distributions of the irradiance obtained in measuring light absorption by Baikal water

N.M. Budnev,¹ G.P. Kokhanenko,² R.R. Mirgazov,¹ and B.A. Tarashchanskii¹

¹ Institute of Applied Physics of Irkutsk State University, Irkutsk

² Institute of Atmospheric Optics, Siberian Branch of the Russian Academy of Sciences, Tomsk

Received November 1, 2005

The operation of an ASP-15 stationary deep-water measuring complex located in the south part of Lake Baikal is analyzed. The complex conducts all-the-year-round measurements of hydrooptical characteristics at 1000–1200-m depths. The method of determining the water absorptivity is based on measuring the decay rate of irradiance from an isotropic emitter as the distance between the source and the receiver changes. Based on numerical modeling of the light field, the method accuracy is estimated and possible causes of anomalous range dependences of the irradiance are determined. The experimental data obtained in recent years with the ASP-15 complex are presented.

Introduction

In 1960, M.A. Markov proposed to use deep natural reservoirs with transparent waters for detecting neutrinos of high energy.³⁰ The first deep-water neutrino telescope¹ NT-200 has been operated in Lake Baikal since 1998. Its effective volume was increased in 2005 due to installation of three additional strings with optical modules.³¹ Also the work is being done on creation of deep-water neutrino telescopes in the Mediterranean Sea.³² Natural water in all these projects is simultaneously both a target substance, with which neutrinos interact, and the medium where the Cherenkov radiation caused by charged relativist particles is emitted and propagates. To correctly analyze the data obtained with neutrino telescopes, it is necessary to have data on the optical parameters of the water medium, which can not be constant in Lake Baikal as in any other natural reservoir.

The ASP-15 instrument (previous name – “Burkhan”⁸) was developed in 1992 for long-term monitoring of the primary optical characteristics in the region of the NT-200 neutrino telescope. All-the-year-round measurements of the optical characteristics of water (absorption and scattering indices and the scattering phase function) are carried out with this device in the wavelength range 350–690 nm at the depth of 1200 m. Measurements of hydrooptical characteristics in the entire layer from the surface to the bottom are carried out in March–April during the period of preventive testing.^{2,33}

All optical parameters of the scattering medium (such as scattering, absorption, and extinction indices) have strict mathematical definitions,^{4–6} that causes the construction of hydrooptical devices intended for precise measurements of these quantities. However, the majority of the known hydrooptical devices⁷ are little suitable for continuous long-term

measurements of hydrooptical parameters *in situ* because of the difficulties related with the impossibility of making precise remote adjustment of narrow light beams and violation of the calibration during measurements. Approximate methods are used in the complex ASP-15 for retrieval of the optical parameters from the light field of a point source.^{9,10} To measure the absorption coefficient, the method is used, the principle of which was proposed for the first time in Ref. 11. It is based on assumption that, in a homogeneous medium, the dependence of the irradiance of a plate on the distance from the source is described by the exponential law with the exponent equal to the absorption coefficient. Analysis of a few years of operation of the ASP-15 complex¹⁰ has shown that the majority of measurements are described by the aforementioned law accurate to about 5%. However, noticeable deviations from this dependence were observed in some cases (as a rule, at extremely high transparency of water), which make it difficult to interpret measurement data. Analysis of the possible errors of the method⁹ is based on the single scattering approximation and the condition of strong anisotropy of scattering, which are not always fulfilled in real measurements.

In this paper we present analysis of operation of the ASP-15 complex based on numerical simulations of the light field of an isotropic source in scattering medium with the optical parameters characteristic of different types of natural waters.

1. Measurement of the absorption coefficient using parameters of light field from a point source

Calculation of the absorption coefficient is based on the known formula for the divergence of the light vector \mathbf{H} ^{12,13}:

$$\operatorname{div}\mathbf{H} = -aE^0, \quad (1)$$

where a is the absorption coefficient, E^0 is the spatial irradiance. The light flux vector \mathbf{H} defined by Gershun¹⁴ is characterized by the fact that its projection on any axis is equal to the difference of irradiances of the plates oriented toward the axis and along the counter direction. If z -axis, as is usually assumed in hydrooptical measurements, has been directed vertically down, then $H_z = E_D - E_U$, E_D and E_U , being, respectively, the irradiances from above and from below. Let us remind that the spatial irradiance in this case is $E^0 = E_D + E_U$. It is very difficult to directly measure the divergence of the vector \mathbf{H} under natural conditions. The formulas for calculating the absorption coefficient using the values, usually measured with the submersible devices (the irradiances E_D and E_U , the vertical extinction coefficient α_a , and the angular distribution of brightness) are also known and were presented by Pelevin.¹⁵ Idealization of the conditions of observations can lead to more simple, but very approximate dependences. For example, Erlov⁵ presented formula for the surface sea layer (horizontal homogeneity) under solar illumination and reasonable assumption that $E_U \ll E_D$

$$E_D = E_0 \exp(-aR), \quad (2)$$

where E_0 is the irradiance at the sea surface, R is the depth of observations. However, use of solar illumination is impossible in the instrumentation intended for deep-water investigations. As a rule, artificial light sources are applied in this case. In the case of point isotropic source in a homogeneous medium only the radial component H_r of the vector \mathbf{H} is not equal to zero, and one can write formula (1) using polar coordinates as follows:

$$\operatorname{div}\mathbf{H} = \frac{1}{r^2} \left[\frac{\partial}{\partial r} (r^2 H_r) \right] = -aE^0 \quad (3)$$

or, as the absolute value $H = H_r$,

$$\frac{dH}{dr} + H \frac{2}{r} = -aE^0. \quad (4)$$

Formula (4) was obtained¹⁶ and reduced to the form containing the parameters measured in hydrooptical experiments:

$$a = \alpha_F(r) \frac{H}{E^0} = \alpha_F(r) \mu(r), \quad (5)$$

where α_F is the extinction coefficient of the flux $F(r) = 4\pi r^2 H(r)$ through a sphere of the radius r surrounding the source; $\mu(r)$ is the mean cosine of the brightness body of radiation at the point r . The simpler way of determining absorption that requires measurement of only irradiance of the plate from the side of the source was proposed in Ref. 11. Let us denote, as before, irradiances of the plates oriented toward the source and along the opposite direction by E_D and E_U . Let us assume that the backscattering is

negligible and, besides, the rate of the change of the backscattered radiation is small:

$$E_U \ll E_D \approx E^0; \quad \frac{dE_U}{dr} \ll \frac{dE_D}{dr}. \quad (6)$$

In this case formula (4) is transformed to

$$\frac{dE_D}{dr} + E_D \frac{2}{r} = -aE_D, \quad (7)$$

where from quite simple law follows for the decrease of irradiance of the plate with the increase of range from the source:

$$E_D = \frac{F_0}{r^2} \exp(-ar). \quad (8)$$

Here F_0 is the light flux emitted by the source. Pelevin¹⁶ has indicated that formula (7) was proposed for the first time by N.G. Boldyrev. Measuring the dependence of irradiance on the range, we determine the absorption from the rate of the decrease of the signal, and the absolute calibration of the device is not needed.

Conditions (6) are sufficient for validity of formula (8), however, they seem to be too strict, and it is impossible to estimate their fulfillment *a priori* without calculations or measurements of the light field. It should be noted, that the law of decrease of irradiance (8) was obtained in Ref. 11 not from Eq. (3) but from general ideas: a) about the decrease of the radiation flux inversely proportional to the square of the range, and b) about exponential dependence of the flux on the value of the true absorption in the medium. Let us consider these items separately.

a) Let us have a conservative medium ($a = 0$). In this case, it follows from Eq. (1) that the absolute value of the light vector $H = E_U - E_D$ is inversely proportional to the square of the distance (energy conservation law). For this formula to hold for the measured component E_D , the condition $E_U \ll E_D$ is sufficient. Prerequisites for this are the following: low backscattering and quite strong absorption, because the flux coming from outside the sphere is absorbed stronger than the direct radiation because of the longer photon free path.

b) the dependence $E_D \sim \exp(-aR)$ is strictly fulfilled at the constant $r = R$ only when prolongation of the photon free path resulting from scattering has been absent. In any case, it is necessary that the fraction of energy transported by the photons whose free path in the medium essentially exceeds the distance between the source and the receiver R should be negligible. This is fulfilled at strongly forward peaked scattering phase functions (not because of simply low backscattering) and/or at significant absorption, because the probability of being absorbed is higher for photons that travel longer.

Thus, both components of formula (8) are valid under the same conditions: strong forward peakedness of the scattering phase function and the significant

true absorption in the medium are necessary. It should be expected that deviations from Eq. (8) can be observed in other cases.

Analysis of data obtained with the ASP-15 device has been attempted in Refs. 2 and 18. The spectral dependence of the absorption coefficient is, on the whole, close to that observed in the ocean water.¹⁷ Variations of the absorption spectra at the depth of 1200 m, on the average, do not exceed 20%. The examples of linear (on logarithmic scale) dependences observed in the majority of measurements and corresponding to the dependence (8) are shown in Fig. 1. The retrieved values of the absorption coefficient are shown next to the lines.

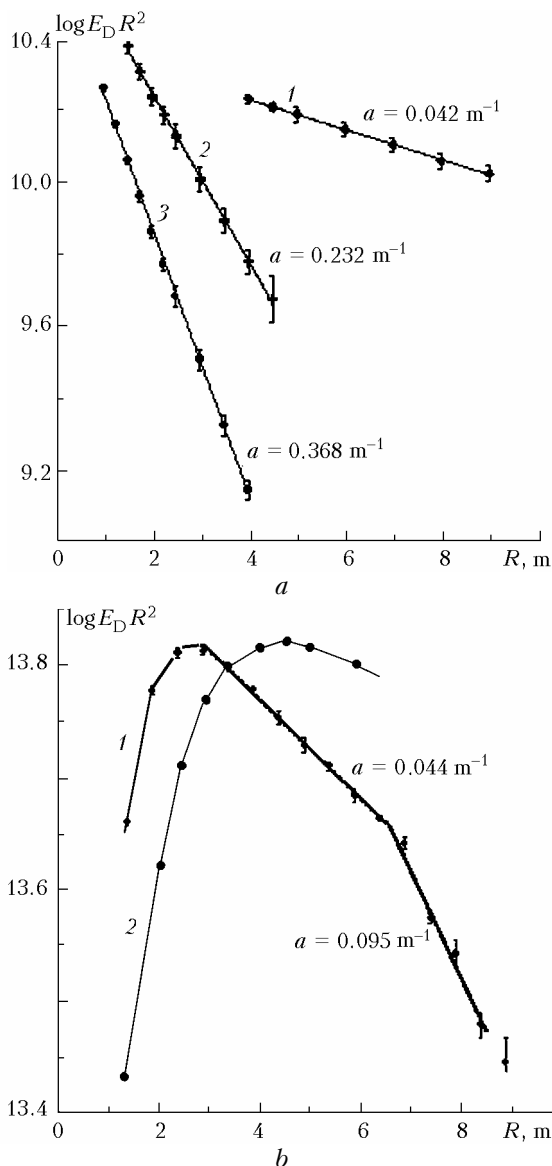


Fig. 1. Experimentally measured dependences of irradiance on the distance from the source: (a) December 27, 1997, depth 850 m. Wavelength $\lambda = 488$ (1); 374 (2); 651 nm (3); (b) July 13, 2001, 1200 m, $\lambda = 488$ nm (1), April 06, 2001, 10 m, $\lambda = 550$ nm (2). Figures at the curves show the values of the absorption coefficient determined from the slope of the lines.

However, some periods of measurements (in 1992, 1997, and 2001), sometimes during a few weeks, quite different curves (Fig. 1b) were observed in the experiments. These are characterized by an increase of $E_D R^2$ with distance at small R and often by the presence of a maximum, after which the exponential decrease occurs again. This happened in the periods when the values of the absorption coefficient were essentially smaller as compared with the typical one. For example, at the wavelength of $\lambda = 488$ nm $a = 0.02 \text{ m}^{-1}$ instead of the typical value 0.05 m^{-1} .

Systematic repetition of such results does not allow explaining them by the instrumentation malfunctioning or by the measurement errors. Obviously, the reason is that the extremely simplified formula (8) is inapplicable in the entire range of variations of the optical parameters of Baikal water. For example, the content of hydrosol in the deep water of the lake is very small. It is seen from measurements with ASP-15 that the value of the scattering coefficient sometimes decreases to 0.01 m^{-1} , that is only four times greater than the molecular scattering coefficient. The contribution of the molecular scattering, which has symmetric scattering phase function, is large under these conditions, and the backscattering is high too. Together with the low absorption, it can lead to violation of the conditions of the Eq. (8) validity. Let us consider below, at which optical parameters of water the anomalous dependences of the type shown in Fig. 1b can be observed, and what errors can appear in the measured absorption coefficient.

2. Algorithms for calculating the light field

Simulation of light fields of the isotropic sources was carried out by the Monte Carlo method using the algorithms of local estimation^{19,20} for the non-stationary transfer equation. It is supposed that the point source $P_0(r, t) = \delta(r)\delta(t)$ of the unit intensity is situated in the homogeneous infinite scattering medium characterized by the scattering coefficient b , absorption coefficient a , and the scattering phase function $g(\gamma) = \beta(\gamma)/b$ ($\beta(\gamma)$ is the coefficient of directional scattering, γ is the scattering angle). A point receiver with the cosine diagram of receiving is at the distance R from it (in real experiment R varies from 0.2 to 10 m). The received light flux is written in the form

$$P(t) = \int_{2\pi} L(t) \cos\phi d\Omega,$$

where $L(t)$ is the irradiance at the point of receiving, and it determines the time behavior of the signal or, in another notation, the photon distribution over the free paths $l = vt$ ($v = 0.224 \text{ m/ns}$ is the light speed in water). The first photons reach the receiver at the moment $T_0 = R/v$. Radiation incident on the receiver without scattering (direct beam) is not simulated, but calculated by the formula

$$E_{\text{dir}} = \frac{1}{4\pi R^2} \exp(-cR),$$

where c is the extinction coefficient.

The irradiance at the point of the receiver is obtained by means of integration of the flux with respect to time

$$E_D = E_{\text{dir}} + \int_{T_0}^{\infty} P(t) dt.$$

Peculiarities of simulation of the initial direction of the photon flux for the isotropic source are considered in detail in Ref. 26. Calculations were carried out for a conservative medium ($a = 0$). Calculation for the preset absorption was made according to the relationship $P(t, b, a \neq 0) = P(t, b, a = 0) \exp(-avt)$.²² The values of the absorption coefficient were selected in the limits $a = 0.005\text{--}0.5 \text{ m}^{-1}$, that overlaps with the observed range of absorption in the wavelength range $0.4\text{--}0.7 \mu\text{m}$. Four types of the scattering phase functions of sea waters were selected (measured experimentally at different time by O.V. Kopelevich and V.M. Pavlov).²¹ Two scattering phase functions have extreme asymmetry. The least forward peaked scattering phase function g_1 (asymmetry $K = 11$, $\langle \cos\gamma \rangle = 0.788$) was observed in transparent water of Sargasso Sea, the most asymmetric g_4 ($K = 361$, $\langle \cos\gamma \rangle = 0.987$) was observed in the water of Black Sea. The scattering phase functions g_2 ($K = 40$, $\langle \cos\gamma \rangle = 0.924$) and g_3 ($K = 139$, $\langle \cos\gamma \rangle = 0.97$) are typical of the open ocean waters. Besides, the scattering phase function of molecular scattering g_m was used. From 10 to 100 millions of trajectories were used in calculations, depending on the shape of the scattering phase function, the time scale was divided into uniform parts of the histogram on the logarithmic scale (5 points per decade).

Figure 2 shows a typical distribution of photons $P(t)$ over the free paths for different distances R between the source and the receiver in the medium with the scattering phase function g_2 and the value of the scattering coefficient $b = 0.15 \text{ m}^{-1}$.

The abscissa axis is the delay of photons Δt relative to the time of coming of the first photon T_0 . Curves 1–4 correspond to the change of R from 0.2 to 30 m. Dotted line shows the asymptotic dependence $P(t) \sim t^{-3/2}$ typical of the isotropic source²² at long Δt times.

The most characteristic peculiarity of the photon distribution over the free paths shown is its bimodal structure observed at not very high optical thickness in the case of point radiation sources.²³ The delta-shaped peak of radiation at the initial time moments is caused by the prevalence of scattering at small angles at these time moments, which does not lead to any noticeable increase of the photon free paths. The cause of appearance of the second maximum is the diffuse background of multiple scattering that appears at large angles, which is characterized by

noticeable delay relative to the arrival of the first photon.²⁴

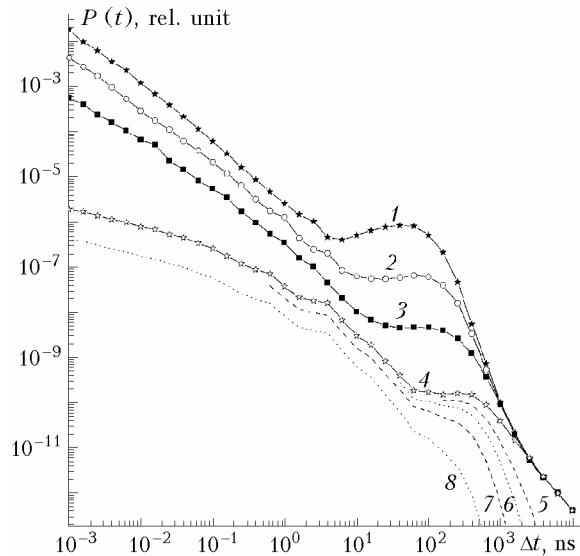


Fig. 2. Light field for different distances between the source and the receiver. Curves 1–4 correspond to $R = 0.2; 1; 5; 30 \text{ m}$. Curves 5–8 correspond to $a = 0.005; 0.01; 0.02; 0.05 \text{ m}^{-1}$ at $R = 30 \text{ m}$.

As was shown,²⁵ irradiation of the back half-sphere (relative to the direction from the source to the receiver) makes significant contribution into it under conditions of infinite scattering medium. The portion of energy falling to this diffuse background is determined by the shape of the scattering phase function and is about 75% for molecular, 30% for the scattering phase function g_2 shown in Fig. 2, and only 4% for the scattering phase function g_4 . It should be noted that this diffuse part of radiation could cause violation of the conditions (6) and lead to the errors in the absorption coefficient measured. Besides, dotted lines in Fig. 2 show the photon distributions for different values of the absorption coefficient (from 0.005 to 0.05 m^{-1}) at $R = 30 \text{ m}$. Even low absorption caused strong attenuation of the photons with long free paths, decreasing the contribution of the diffusely scattered radiation.

3. Formation of the irradiance at the receiver and analysis of the method for measuring the absorption coefficient

The calculated results on the irradiance at different depths in the scattering medium make it possible to consider how the basic assumptions, accepted in the approximation (8), are fulfilled. Let us remind that it is the exponential dependence of the irradiance on the absorption (at a fixed distance R) and the inverse dependence of irradiance on the squared distance.

The most characteristic pattern of formation of the radiation flux at the receiver is observed for the conservative medium, because deviations from the

inverse dependence on the squared range are best pronounced in the absence of absorption. The dependences of some components of irradiance (the direct beam E_{dir} (curve 1), scattered E_{scat} (2), and total E_D (3) fluxes for the medium with the scattering phase function g_1) on the distance are shown in Fig. 3a for the values $a = 0, b = 0.15 \text{ m}^{-1}$.

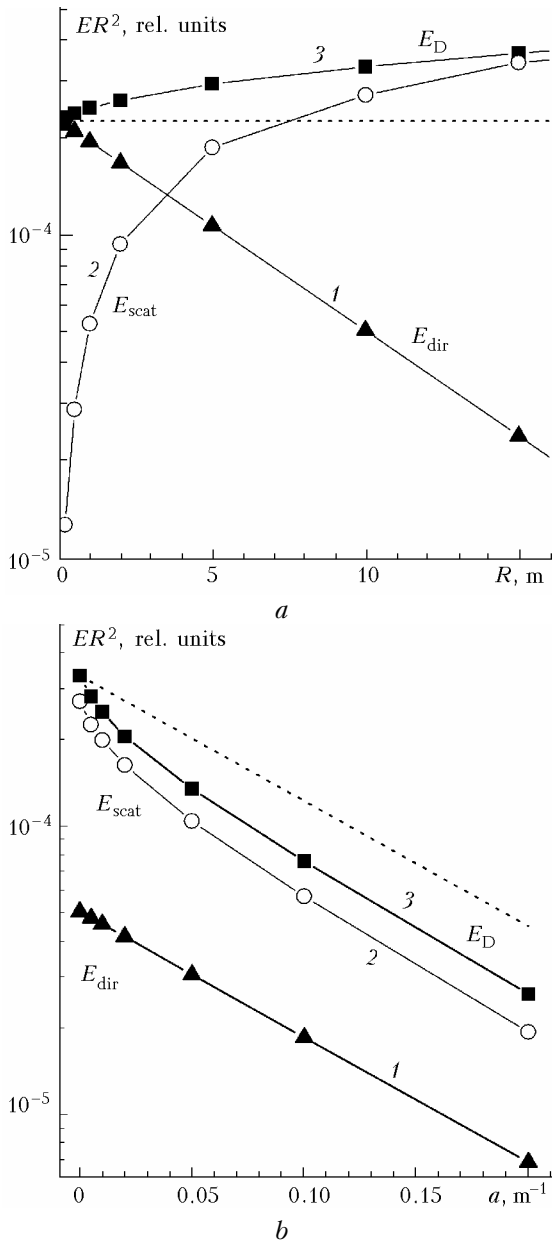


Fig. 3. Formation of the irradiance at the receiver: direct flux (1), scattered flux (2), total flux (3). Medium with the scattering phase function g_1 , $b = 0.15 \text{ m}^{-1}$; (a) medium without absorption, (b) effect of absorption at $R = 10 \text{ m}$.

All the calculated parameters in Fig. 3 are multiplied by the squared distance R^2 . The value of the light flux $HR^2 = (E_D - E_U)R^2$ in this case should be constant (dotted line in Fig. 3a). It is seen that as the distance R increases, the direct flux decreases as $E_{dir}R^2 = \exp(cR)$, while the portion of the scattered

flux E_{scat} increases. The total irradiance E_D also increases, and the excess of the value $E_D R^2$ over a constant one is determined by the back flux E_U that is ignored in Eq. (8). As should be expected, this excess is best pronounced in the case of weakly asymmetric scattering phase functions.

The dependences of the direct (curve 1), scattered (curve 2), and total (curve 3) fluxes on the absorption coefficient a are shown in Fig. 3b for the fixed distance $R = 10 \text{ m}$. The direct flux exponentially decreases with the absorption increase. Irradiance for $R = 10 \text{ m}$ is mainly determined by the scattered radiation, which significantly exceeds the direct flux. As the absorption coefficient increases, more fast than $\exp(-aR)$ decrease of the irradiance is observed (dotted line in Fig. 3b). It is caused by predominant attenuation of the photons with longer travel paths. (Let us remind that the increase of the photon travel paths in Eq. (8) is ignored). Then (at $a > 0.1 \text{ m}^{-1}$) the rate of decrease approaches the exponential one, but the resulting underestimation of the signal ($\approx 30\%$) remains. The direct flux at small R is significantly greater than the scattered one, and deviations from the exponent are less noticeable. As a result, underestimation of the signal increases with the distance R , and it can lead to overestimation of the absorption coefficient.

The dependences of the value $E_D R^2$ on the distance, which are of interest from the practical point of view, from which the absorption is determined in measurements by means of the ASP-15 device, are shown in Fig. 4 for the media with different scattering phase functions (including molecular) and for the values $a = 0.02 \text{ m}^{-1}$, $b = 0.15 \text{ m}^{-1}$, $\Lambda = b/c = 0.88$.

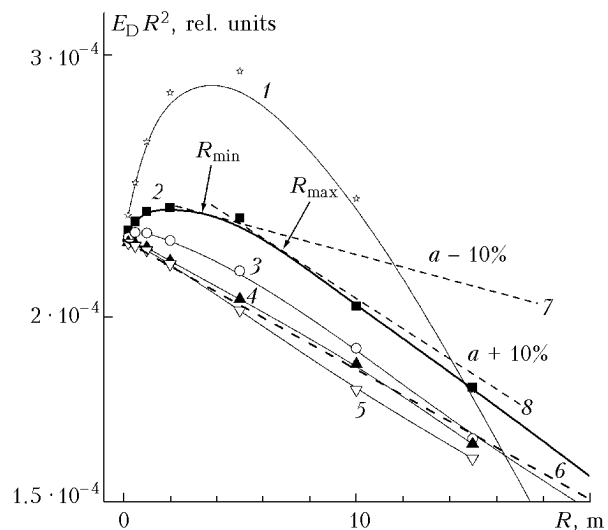


Fig. 4. Irradiance as a function of the distance. Curves 1–5 correspond to the scattering phase functions g_m, g_1, \dots, g_4 . Dotted lines shows the dependence $\exp(-aR)$ for the true value a (6) and different from the true value by $\pm 10\%$ (7, 8).

Maximum of the dependence $E_D(R)$ is well pronounced for the weakly asymmetric scattering

phase functions. It is similar to that, which is sometimes observed in experiments (see Fig. 1*b*). The maximum moves to the left at increase of the asymmetry of the scattering phase function.

It is unnoticeable for the scattering phase function with maximum asymmetry, and the decrease begins from zero. The value of the maximum decreases at increasing absorption coefficient, and at $a = 0.5 \text{ m}^{-1}$ ($\Lambda = 0.23$) it does not exceed 1% relative to the exponent. The decrease becomes exponential at large distances for all scattering phase functions, but the slope is overestimated at large distances. The greatest overestimation is observed at low absorption and weakly asymmetric scattering phase functions. The value of the measured absorption coefficient only rarely exceeded 10% for the range of simultaneous variability of the asymmetry K and the albedo Λ (see Fig. 5 below) observed in water of Lake Baikal.

The presence of the maximum of the dependences $E_D(R)$ (similar to that shown in Fig. 4) imposes restrictions on the distances, at which measurements of the absorption coefficient are possible with acceptable accuracy. Indeed, the slope of the curves after passing the maximum gradually increases with the increase of the distance from the source. Dotted line 7 in Fig. 4 has the slope, which is 10% less than the true absorption coefficient and is tangent to the curve 2 at the point R_{\min} . Starting from this distance, underestimation of the measured absorption coefficient becomes less than the preset value $\Delta a = 10\%$. Deviations from the exponent do not exceed $\pm \Delta a$ at some distances, but then after $R > R_{\max}$ overestimation of the slope of the curve (and, hence, the measured value) exceeds Δa (line 8).

It is clear from the data presented, that restrictions are essential for weakly asymmetric scattering phase functions and low absorption. The range where $R_{\min} - R_{\max}$ obey the approximation (8) is very narrow for the molecular scattering phase function. The range becomes wider with the increase of the asymmetry of the scattering phase function, and the restriction from the side of large distances becomes essential only for weakly asymmetric scattering phase functions of the type g_1 and g_2 . Restrictions from the side of small distances are essential for all scattering phase functions, and R_{\min} increases with the increase of the albedo ($\Lambda \rightarrow 1$).

The results shown in Fig. 4 were obtained at the scattering coefficient set to be $b = 0.15 \text{ m}^{-1}$ characteristic of the transparent near-surface water of Baikal in February and March. The similarity relationships^{4,22} known in the theory of radiation transfer make it possible to obtain the dependences of the light flux for other values of the scattering coefficient b by means of simple replacement of the scales, leaving invariant the dimensionless optical parameters, the optical thickness $\tau = cR$ and the single scattering albedo $\Lambda = b/c$.

The plot in dimensionless coordinates is shown in Fig. 5, which shows the minimum values of the optical depth $\tau_{\min} = R_{\min}(a + b)$, starting from which the calculated underestimation of the absorption

coefficient is less than 10%. The abscissa axis presents the value $1 - \Lambda$, the ordinate axis is the asymmetry of the scattering phase function K . Figures at the lines show the values τ_{\min} .

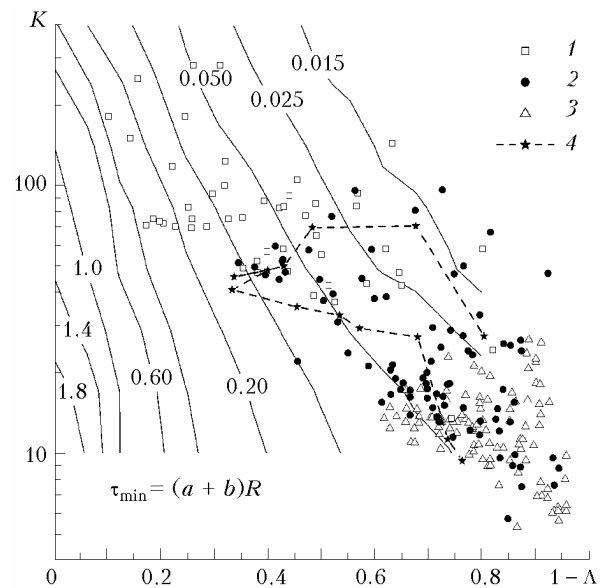


Fig. 5. Minimum optical thickness, for which the approximation (8) is fulfilled with the error less than 10%. Signs show combinations of the parameters K and Λ observed in simultaneous measurements at the depth 0–100 (1); 200–600 (2); 1000–1200 m (3).

Figure 5 confirms the regularity proposed earlier: the less is the asymmetry of the scattering phase function and the lower is the absorption (lower left corner of the plot), the greater is the distance, starting from which the rate of decrease of the irradiance satisfies Eq. (8). The signs show combinations of the parameters (K, Λ) observed during some years. For the majority of situations $\tau_{\min} \ll 1$, and the “correct” exponential dependence is observed along the entire measurement path. Anomalous dependences (of the type of Fig. 1*b*) appear at falling the optical parameters to the left area of the plot in Fig. 5 with very high value of the albedo Λ . As the ASP-15 instrument is capable of measuring all necessary optical parameters (as concerning the accuracy of measuring the asymmetry of scattering see Ref. 25), there is a possibility of controlling the conditions of the approximation (8) validity and to avoid essential errors in measurements of the absorption coefficient.

4. Experimental data on the optical parameters of water

The data of some measurements carried out with an ASP-15 device in 2001–2005 are shown in Figs. 5 and 6. Correlation between two simultaneously measured optical parameters is shown in Fig. 5: asymmetry of the scattering phase function K and the single scattering albedo $\Lambda = b/c$ observed in water of Lake Baikal.

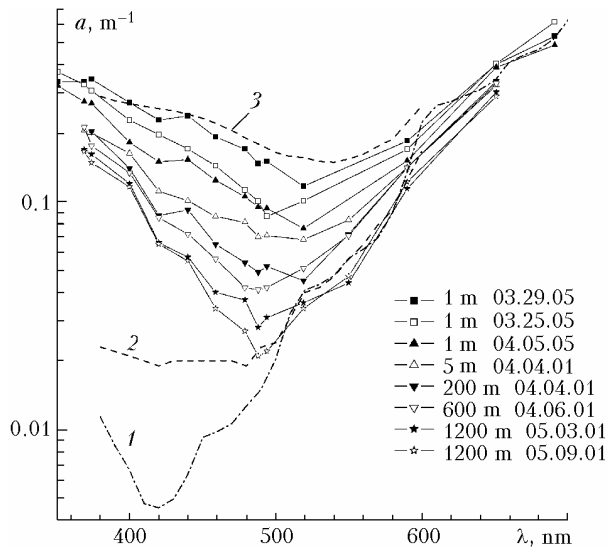


Fig. 6. Variability of the absorption spectra of water of Lake Baikal at different depths.

Measurement data shown are grouped by depth; points corresponding to the change of the wavelength from 351 to 690 nm from the same series of observation are connected by the dashed line (March 16, 2001, curve 4). Similar dependence is also characteristic of other series. Asymmetry of the scattering phase function mainly increases with wavelength with the extremely small Λ values being characteristic of the edge (red and violet) wavelength ranges. The well pronounced correlation between two parameters is easily explained if one takes into account that the dynamics of the optical parameters in the water far from the coast is caused mainly by the development of large organic particles (plankton), for which variability of the scattering coefficient is significantly greater than that of the absorption coefficient. Weakly asymmetric scattering phase functions (of the type g_1) are characteristic of transparent (deep) waters with small content of hydrosol. Light scattering in this case is low and the value Λ is small too. Large Λ values can be observed in turbid water with enhanced content of large organic particles, but in this case the scattering phase function is characterized by strong asymmetry (scattering phase functions of the types g_3 and g_4).

The absorption spectra for different depths are shown in Fig. 6. Dotted line 1 shows the absorption spectrum of pure water obtained under laboratory conditions.²⁷ It is seen that as depth increases, absorption increases mainly in the shortwave range (due to the dissolved organic substance), the minimum of absorption moves from 488 to 520 nm. Three upper curves related to the depth of 1 m show quite strong variability of the absorption spectrum during a few days in the near-surface layer of the lake. On the whole, the spectral dependence of absorption is close to the known dependences characteristic of the open ocean waters.¹⁷ An example of absorption spectrum for the water of open ocean is also shown here. It was obtained by Pelevin and Rostovtseva²⁹ for the case of oligotrophic (curve 2, the value of the optical

index of the type of water $m = 1.5$) and eutrophic water (3, $m = 9$). It is seen that absorption in the shortwave range in water of Lake Baikal increases significantly faster than in the ocean water.

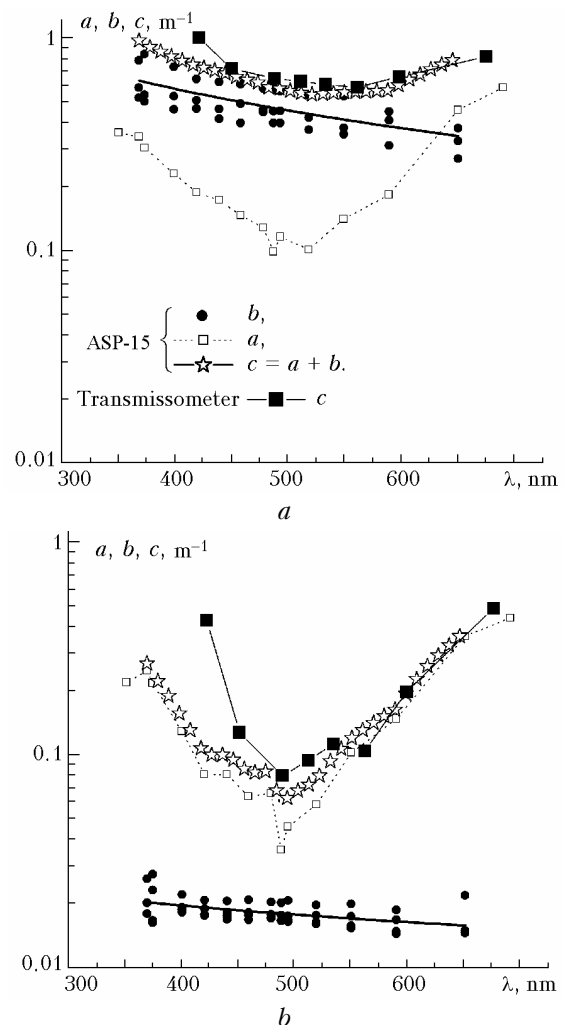


Fig. 7. Comparison of the results obtained when measuring water transparency with two devices. Depth of 5 (a) and 1000 m (b).

Comparison of the results of simultaneous measurements of the optical parameters in April 2005 with an ASP-15 device and submersible photometer – transmissometer²⁷ is shown in Fig. 7. The transmissometer measures directly the extinction coefficient c (shown by black squares), extinction from the data of ASP-15 is obtained by summing the scattering and absorption $c = a + b$ (asterisks). Mean spectral behavior of the scattering index a few days before measurements at the preset depth is taken (black circles). It is seen that the data of independent measurements well coincide in the long-wave range, however, there is essential difference in the range of 420 nm. The reason of such discrepancies has not been clarified yet. It is characteristic that the spectral behavior at the depth of 5 m has the form $b \sim \lambda^{-1.04}$, that agrees with the O.V. Kopelevich model of the scattering properties of water.¹⁷

Conclusions

The method for measuring the absorption coefficient of a scattering medium considered in this paper is based on the assumption of low backscattered radiation and negligible increase of the photon free paths due to multiple scattering. The calculated results show that these assumptions can be violated at some values of hydrooptical parameters. The especially noticeable anomalies lying in non-monotonic behavior of the value $E_D R^2$ (the product of irradiance of the plate to the square of the distance between the source and the receiver) can be observed at simultaneous fulfillment of two conditions: weak asymmetry of the scattering phase function and low absorption. Such a situation is possible in measurements in deep zone of Lake Baikal, where water can be very transparent, and asymmetry of scattering is small because of the absence of large organic particles. It can be the most pronounced in the wavelengths range of 480–520 nm, where absorption is minimum, and in the wavelength range of 690 nm, where dramatic increase of asymmetry of scattering is sometimes observed.²⁵ At the same time, the most probable combinations of the optical parameters like asymmetry of scattering and single scattering albedo observed in water of Lake Baikal allow one to say that the conditions (6) hold in the majority of cases, for which the described method of measuring the absorption coefficient provides adequate results and can be employed in the long-term monitoring of the optical properties of Baikal water.

Acknowledgments

Authors would like to thank G.V. Domogatskii for his attention and interest in this study.

The work was supported in part by Program 6.3 of the Department of Earth's Sciences of the RAS (project "Study of atmospheric pollutions and surface water of Lake Baikal") and Russian Foundation for Basic Research (grants No. 04-02-16171 and 05-02-31004k).

References

1. *Baikal Neutrino Collaboration. The Baikal Underwater Neutrino Telescope: Design, Performance, and First Results*, *Astropart. Phys.* **7**, Issue 3, 263–282 (1997).
2. N.M. Budnev, R.R. Mirgazov, and B.A. Tarashchansky, in: *Proc. of V Workshop on Phys. Processes in Natural Waters*, ed. by S. Semovski (Limnological Inst., Irkutsk, 2000), pp. 59–62.
3. P.P. Sherstyankin, *Experimental Investigations of the Light Field in Lake Baikal* (Nauka, Moscow, 1975), 90 pp.
4. A.P. Ivanov, *Basics of the Hydrooptics* (Nauka i Tekhnika, Minsk, 1975), 504 pp.
5. N. Erlov, *Sea Optics* (Mir, Moscow, 1970), 224 pp.
6. M.V. Kozlyaninov, in: *Atmospheric and Ocean Optics* (Nauka, Moscow, 1981), 230 pp.
7. V.I. Burenkov, B.F. Kelbalikhanov, and O.V. Kopelevich, in: *Ocean Optics*. Vol. 1. *Physical Ocean Optics* (Nauka, Moscow, 1983), pp. 114–149.
8. B.A. Tarashchanskii, R.R. Mirgazov, and K.A. Pocheikin, *Atmos. Oceanic Opt.* **8**, No. 5, 401–403 (1995).
9. O.N. Gaponenko, R.R. Mirgazov, and B.A. Tarashchanskii, *Atmos. Oceanic Opt.* **9**, No. 8, 677–682 (1996).
10. L.B. Bezrukov, N.M. Budnev, M.D. Galperin, J.-A.M. Jilkibaev, O.Yu. Lanin, and B.A. Tarashchanskii, *Okeanologiya* **30**, No. 6, 1022–1026 (1990).
11. D. Bauer, J.C. Brun-Cottan, and A. Saliot, *Cah. Oceanogr.* **23**, No. 9, 841–858 (1971).
12. A.A. Gershun, *Tr. S.I. Vavilov State Optical Institute* **4**, Issue 38 (1928).
13. N.G. Boldyrev, *Tr. S.I. Vavilov State Optical Institute* **6**, Issue 59 (1931).
14. A.A. Gershun, *Dokl. Akad. Nauk SSSR* **49**, No. 8, 578 (1945).
15. V.N. Pelevin, *Izv. Akad. Nauk SSSR, Ser. Fiz. Atmos. Okeana* **1**, No. 5, 539–544 (1965).
16. V.N. Pelevin and T.M. Prokudina, in: *Atmospheric and Oceanic Optics* (Nauka, Leningrad, 1972), pp. 148–157.
17. O.V. Kopelevich, in: *Ocean Optics*. Vol. 1. *Physical Ocean Optics* (Nauka, Moscow, 1983), pp. 166–208.
18. N.M. Budnev, G.P. Kokhanenko, R.R. Mirgazov, I.E. Penner, B.A. Tarashchansky, V.S. Shamanaev, P.P. Sherstyankin, V.V. Blinov, and V.G. Ivanov, in: *Current Problems in Optics of Natural Waters*. I. Levin and G. Gilbert, eds., *Proc. of D.S. Rozhdestvensky Optical Society*, St. Petersburg (2001), pp. 318–322.
19. G.I. Marchuk, G.A. Mikhailov, M.A. Nazaraliev, R.A. Darbinyan, B.A. Kargin, and B.S. Elepov, *Monte Carlo Method in Atmospheric Optics* (Nauka, Novosibirsk, 1976), 284 pp.
20. G.M. Krekov, G.A. Mikhailov, and B.A. Kargin, *Izv. Vyssh. Uchebn. Zaved. SSSR, Ser. Fizika*, No. 4, 5–10 (1968).
21. A.M. Gurfink, in: *Light Fields in the Ocean* (Institute of Oceanology RAS, Moscow, 1980), pp. 115–165.
22. E.P. Zege and I.L. Katsev, *Image Transfer in a Scattering Medium* (Nauka i Tekhnika, Minsk, 1985), 326 pp.
23. G.P. Kokhanenko and V.A. Krutikov, in: *Abstracts of Reports at the Conference on Numerical Methods for Solving the Transfer Equation*, Tartu (1988), pp. 98–101.
24. V.V. Vergun, E.V. Genin, G.P. Kokhanenko, V.A. Krutikov, and D.S. Mezhevoi, *Atm. Opt.* **3**, No. 9, 845–851 (1990).
25. N.M. Budnev, G.P. Kokhanenko, M.M. Krekova, I.E. Penner, V.S. Shamanaev, R.R. Mirgazov, and B.A. Tarashchanskii, *Atmos. Oceanic Opt.* **18**, Nos. 1–2, 96–104 (2005).
26. G.P. Kokhanenko, B.A. Tarashchansky, N.M. Budnev, and R.R. Mirgazov, *Proc. SPIE* **6160**, Part 2, 64–76 (2005).
27. P.P. Sherstyankin, G.P. Kokhanenko, I.E. Penner, A.P. Rostov, L.N. Kuimova, V.G. Ivanov, and V.V. Blinov, *Dokl. Ros. Akad. Nauk* **383**, No. 1, 106–110 (2002).
28. R.M. Pope, and E.S. Fry, *Appl. Opt.* **36**, No. 33, 8710–8722 (1997).
29. V.N. Pelevin and V.V. Rostovtseva, *Atmos. Oceanic Opt.* **10**, No. 9, 617–621 (1997).
30. M.A. Markov, in: *Proc. 1960 Annual Int. Conf. on High Energy Phys.* (Rochester, 1960), p. 578.
31. *Baikal Neutrino Collaboration. The BAIKAL Neutrino Project: Status, Results, and Perspectives*, *Nuclear Physics B* **143**, 335–342 (2005).
32. L.K. Resvanis, ed., *Proc. 3rd NESTOR Int. Workshop* (Pylos, Greece, 1993).
33. V.I. Dobrynin and B.A. Tarashchanskii, in: *Abstracts of Reports at 11th Plenum on Ocean Optics* (Institute of Physics, Krasnoyarsk, 1990), Part 1, pp. 89–90.